

Spin tomography

G M D'Ariano¹, L Maccone^{1,2} and M Piani¹

¹ Quantum Optics and Information Group, INFN Udr Pavia, Dipartimento di Fisica 'Alessandro Volta' and INFN, Via Bassi 6, 27100 Pavia, Italy

² Massachusetts Institute of Technology, Research Laboratory of Electronics, MIT 36-497, Cambridge, MA 02139, USA

Received 13 October 2002

Published 29 January 2003

Online at stacks.iop.org/JOptB/5/77

Abstract

We propose a tomographic reconstruction scheme for spin states. The experimental set-up, which is a modification of the Stern–Gerlach scheme, can be easily performed with currently available technology. The method is generalized to multiparticle states, analysing the spin-1/2 case for indistinguishable particles. Some Monte Carlo numerical simulations are given to illustrate the technique.

Keywords: Quantum tomography, state reconstruction, quantum measurement, spin states, composite systems

(Some figures in this article are in colour only in the electronic version)

1. Introduction

The main idea of tomography is to reconstruct the density matrix ρ or, equivalently, the expectation value of any observable of the system from repeated measurements on an ensemble of identical states. In this paper a 'spin tomography' for reconstructing spin states is developed in the framework of generalized tomography, starting from group theory [1]. There have been other proposals to infer the spin state [2]. Our method is both easy to carry out experimentally and, for the first time, allows also a reconstruction of indistinguishable multiparticle spin-1/2 states, which is quite general since it encompasses a vast class of experimentally accessible systems.

The best known quantum tomographic procedure is optical homodyne tomography [3], for the reconstruction of the density matrix ρ_r of the radiation field from the homodyne probability $p(x, \phi)$. It is based on the following formula [4]:

$$\rho_r = \int_0^\pi \frac{d\phi}{\pi} \int_{-\infty}^{+\infty} dx p(x, \phi) K(x - x_\phi), \quad (1)$$

where x_ϕ is the quadrature operator and $K(x)$ is an appropriate kernel function. We will not go into details about this formula, as we only want to stress the analogy with the spin case. In fact, consider the spin density operator ρ , which is defined on a Hilbert space \mathcal{H}_s of dimension $2s + 1$. We will prove the following formula:

$$\rho = \sum_{m=-s}^s \int \frac{d\vec{n}}{4\pi} p(\vec{n}, m) K_s(m - \vec{s} \cdot \vec{n}), \quad (2)$$

where the integral is performed over all directions of the vector \vec{n} , $p(\vec{n}, m)$ is the probability of having outcome m measuring the self-adjoint operator $\vec{s} \cdot \vec{n}$ (\vec{s} being the spin operator) and $K_s(x)$ is a kernel function that will be defined later.

It is possible to show that both equations (1) and (2) follow from a single operator identity, derived using group theory. In fact, define tomographic group G as an unimodular group (i.e. left and right invariant measure are coincident) which has a unitary irreducible square-integrable representation $\mathcal{R}(g)$ ($g \in G$) on the Hilbert space \mathcal{H} of the physical system. (A square-integrable representation is such that $\int dg |\langle u | \mathcal{R}(g) | v \rangle|^2 < \infty$, where the integral is extended to all the elements g of the group G , dg is an invariant measure for G , and where the integral is not dependent on the choice of $|u\rangle, |v\rangle \in \mathcal{H}$ (as will be shown later).) The operator identity we derive (1) and (2) from, and which is valid for any tomographic group G , is the following:

$$\rho = \int dg \text{Tr}[\rho \mathcal{R}(g)] \mathcal{R}^\dagger(g), \quad (3)$$

valid for any trace class operator ρ acting on \mathcal{H} . This formula, derived from general considerations in [1, 5], is derived also in the appendix using only group theory.

The outline of the paper is as follows. In section 2, the tomography procedure to reconstruct the spin state of single-particle systems is introduced and analysed. The experimental set-up is described and some demonstrative numerical simulations of the procedure are studied. In section 3 the extension to the reconstruction of multiparticle spin states is studied. For distinguishable particles, the general reconstruction procedure

is given while, for indistinguishable particles, the cases of two and three spin-1/2 particles is analysed in detail. In section 4 the orders of magnitude of possible experimental set-ups are discussed, showing the feasibility of the proposed method. In the appendix the group tomography is derived by proving the tomographic reconstruction formula (3) in the framework of group theory.

2. Single-particle spin tomography

Starting from the general operator identity (3), we now specify the physical system as a single spin. In this case $\mathcal{H} = \mathbb{C}^{2s+1}$, s being the spin of the particle. For such a system, we can choose the group $SU(2)$ of 2×2 unitary matrices with unit determinant as the tomographic group G . In fact, $SU(2)$ can be parametrized through the ‘rotation parameters’ (\vec{n}, ψ) —where $\vec{n} = (\cos \varphi \sin \vartheta, \sin \varphi \sin \vartheta, \cos \vartheta)$, $\vartheta \in [0, \pi]$, $\varphi \in [0, 2\pi]$ and $\psi \in [0, 2\pi]$ —and it induces a unitary irreducible representation on \mathbb{C}^{2s+1} . The operators constituting this representation are given by

$$\mathcal{R}(\vec{n}, \psi) = e^{i\vec{s} \cdot \vec{n} \psi}, \quad (4)$$

where \vec{s} is the particle spin operator. Haar’s invariant measure³ for $SU(2)$ is, with this parametrization and with the normalization needed for the invariant measure (see the appendix),

$$d\mathcal{g}(\vec{n}, \psi) = \frac{2s+1}{4\pi^2} \sin^2 \frac{\psi}{2} \sin \vartheta \, d\psi \, d\vartheta \, d\varphi. \quad (5)$$

As will be seen in the following, the choice of $SU(2)$ as tomographic group G is not unique for a spin system. It is easy to obtain the spin tomography (2) starting from equation (3), which we now rewrite as

$$\begin{aligned} \varrho &= \frac{(2s+1)}{4\pi^2} \int_0^{2\pi} d\psi \sin^2 \frac{\psi}{2} \int_0^\pi d\vartheta \sin \vartheta \\ &\times \int_0^{2\pi} d\varphi \operatorname{Tr}[\varrho e^{i\vec{s} \cdot \vec{n} \psi} e^{-i\vec{s} \cdot \vec{n} \psi}]. \end{aligned} \quad (6)$$

Evaluating the trace over the complete set of vectors $|\vec{n}, m\rangle$ (which are the eigenstates of $\vec{s} \cdot \vec{n}$, relative to the eigenvalue m), we find equation (2), by defining

$$K_s(x) \doteq \frac{(2s+1)}{\pi} \int_0^{2\pi} d\psi \sin^2 \frac{\psi}{2} e^{i\psi x}, \quad (7)$$

and by noticing that $\langle \vec{n}, m | \varrho | \vec{n}, m \rangle = p(\vec{n}, m)$.

It should be pointed out that formula (1) for optical homodyne tomography can be proven from equation (3) with a very similar argument.

How do we use formula (2)? In order to measure the matrix elements $\varrho_{il} = \langle a_i | \varrho | a_l \rangle$ for all i, l ($\{|a_i\rangle\}$ being a basis for \mathcal{H}_s), we only need to calculate $\langle a_i | K_s(m - \vec{s} \cdot \vec{n}) | a_l \rangle$ and to measure $p(\vec{n}, m)$.

The most convenient choice for the basis $\{|a_i\rangle\}$ is the set $\{|m\rangle\}$ of eigenvectors of s_z ($m = -s, \dots, s$). Thus, the

³ Haar’s measure $d\mu(g)$ must be such that $\int d\mu(g) = 1$, and $\forall h \in \mathcal{G}$, $d\mu(g) = d\mu(h \cdot g) = d\mu(g \cdot h)$.

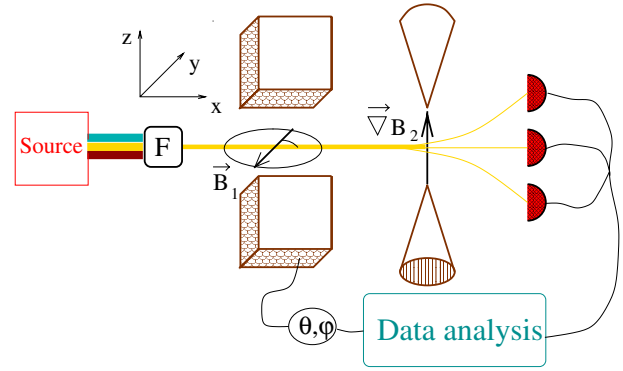


Figure 1. Experimental apparatus for spin tomography. The Fizeau filter (F) selects particles with the same velocity from an incoming beam. These are then injected into a magnetic field \vec{B}_1 , which forms an angle φ with the y axis and has intensity proportional to ϑ . For the tomographic reconstruction the phases ϑ and φ need to be varied during the experiment. The remaining part of the apparatus is a conventional Stern–Gerlach scheme (in the figure we show the case of spin $s = 1$ as an example). A computer finally correlates the experimental results with the parameters ϑ and φ in order to reconstruct the density matrix, according to equation (6).

calculation of the matrix elements of the kernel operator, by defining $\lambda_{l,m} \doteq \langle l | \vec{n}, m \rangle$, yields

$$\begin{aligned} \langle i | K_s(m - \vec{s} \cdot \vec{n}) | l \rangle &= \frac{(2s+1)}{\pi} \int_0^{2\pi} d\psi \sin^2 \frac{\psi}{2} \\ &\times \sum_{m'=-s}^s e^{i\psi(m-m')} \lambda_{i,m'} \lambda_{l,m'}^* \\ &= (2s+1) \left(\lambda_{i,m} \lambda_{l,m}^* - \frac{\lambda_{i,m+1} \lambda_{l,m+1}^* + \lambda_{i,m-1} \lambda_{l,m-1}^*}{2} \right). \end{aligned}$$

Observing that

$$|\vec{n}, m\rangle = e^{-i\vartheta \vec{s} \cdot \vec{n}_\perp} |m\rangle, \quad (8)$$

with $\vec{n}_\perp \doteq (-\sin \varphi, \cos \varphi, 0)$, the evaluation of $\lambda_{l,m}$ is given by

$$\begin{aligned} \lambda_{l,m} &= \langle l | e^{i\vartheta(\sin \varphi s_x - \cos \varphi s_y)} | m \rangle = \langle l | e^{-i\varphi s_z} e^{-i\vartheta s_y} e^{i\varphi s_z} | m \rangle \\ &= e^{i\varphi(m-l)} \sqrt{(s+m)!(s-m)!(s+l)!(s-l)!} \\ &\times \sum_\nu \frac{(-1)^\nu (\cos \frac{\vartheta}{2})^{2s+m-l-2\nu} (-\sin \frac{\vartheta}{2})^{l-m+2\nu}}{(s-l-\nu)!(s+m-\nu)!(\nu+l-m)! \nu!}, \end{aligned} \quad (9)$$

where the sum is performed over the values of ν for which the argument of the factorials is non-negative. In the last equality we used Wigner’s formula [6].

2.1. Experimental set-up and state reconstruction procedure

We now describe the method to measure the state ϱ of an ensemble of non-charged particles, giving the details of the experimental apparatus, depicted in figure 1. The beam of particles impinges onto a Fizeau filter, which selects one velocity (in the x direction) for the particles. This is needed in order to ensure that each particle spends the same amount of time t in the following region where a magnetic field \vec{B}_1 is present. The field \vec{B}_1 , which is parallel to the xy plane, is chosen so that $\vec{B}_1 = B_1 \vec{n}_\perp = B_1(-\sin \varphi, \cos \varphi, 0)$. In this way, its effect on the spin state ϱ results in the unitary transformation $U^\dagger \varrho U$, with

$$U = \exp[i\gamma B(\sin \varphi s_x - \cos \varphi s_y)t]. \quad (10)$$

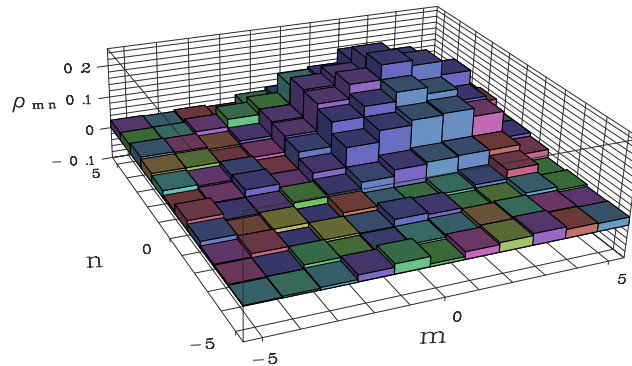


Figure 2. Simulation of the reconstruction of the density matrix for a coherent spin state ρ_{coh} . The parameters for the state are $\alpha = 1$ and $s = 5$. The simulation is performed using 3000 spin measurements to generate the density matrix.

Equation (10) follows from the Hamiltonian $H = -\vec{\mu} \cdot \vec{B}$, with $\vec{\mu} \doteq \gamma \hbar \vec{s}$ ($\vec{\mu}$ being the intrinsic magnetic moment of the particle and γ its gyromagnetic factor). Successively, the particles cross a gradient of magnetic field \vec{B}_2 , whose effect is to split the beam, giving a measure of s_z for the state $U^\dagger \rho U$, as in a Stern–Gerlach experiment. In this way we obtain the probability $\langle m | U^\dagger \rho U | m \rangle$, which is equal to $p(\vec{n}, m)$ by choosing $B_1 = -\vartheta/(\gamma t)$, and by using equation (8). Therefore, by controlling the field \vec{B}_1 , we obtain $p(\vec{n}, m)$ for all \vec{n} . In fact, the direction of \vec{B}_1 selects φ , while its intensity B_1 selects ϑ . Now, in order to reconstruct the density matrix ρ , only data analysis is needed, i.e. the insertion of the measured $p(\vec{n}, m)$ into equation (2). One may object that an infinite number of measures are required. However, the calculation of the integral in (2) with Monte Carlo techniques guarantees that the reconstructed matrix elements are affected by statistical errors only, which can be made arbitrarily small by increasing the number of measures. In practice, a rather small number of data is required to obtain negligible errors, as we will show by numerically simulating the experiment.

We first simulate the case of a coherent spin state [7], i.e.

$$|\alpha\rangle_s \doteq e^{\alpha s_+ - \alpha^* s_-} | -s \rangle, \quad \alpha \in \mathbb{C} \quad (11)$$

where $s_\pm \doteq s_x \pm i s_y$. Notice the similarity with the customary optical coherent state, defined as $|\alpha\rangle \doteq e^{\alpha a^\dagger - \alpha^* a} | 0 \rangle$, where a is the annihilator operator for the optical mode and $| 0 \rangle$ is the vacuum state. In figures 2 and 3 we show the reconstructed density matrix $\rho_{coh} = |\alpha\rangle_s \langle \alpha|$ resulting from a Monte Carlo simulated experiment.

As an additional example, in figures 4 and 5 we give the simulated reconstruction of a thermal spin state, which is the mixture defined by

$$\rho_{th} \doteq \frac{e^{-\epsilon s_z}}{\text{Tr}[e^{-\epsilon s_z}]}, \quad \epsilon \in \mathbb{R}. \quad (12)$$

The state ρ_{th} describes a gas of non-interacting spins in thermal equilibrium with a reservoir at a temperature T and in the presence of a magnetic field B_z parallel to the z axis, i.e. $\epsilon = -\gamma \hbar B_z / (k_B T)$, k_B being the Boltzmann constant.

2.2. Discrete spin tomography

Up to now $SU(2)$ has been used as the tomographic group G for the reconstruction of the spin density matrix. This choice for

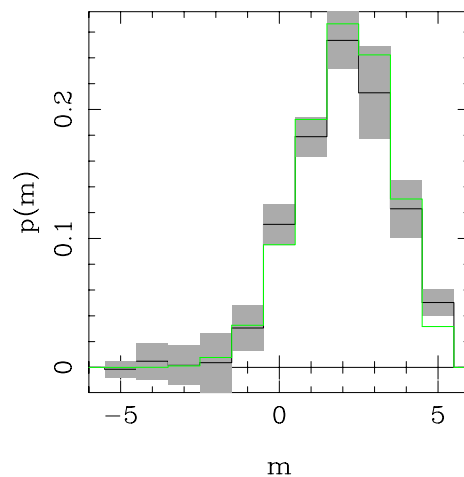


Figure 3. Diagonal elements of the matrix given in figure 2. The statistical error bars are obtained by dividing the measurements into 10 statistical blocks. The full line indicates the theoretical value.

G is not unique. For example, in the case of spin $s = 1/2$, it is possible to also use the group defined as $\mathcal{G} \doteq \{i\vec{\sigma}, -i\vec{\sigma}, I, -I\}$, where $\vec{\sigma}$ is the vector of Pauli matrices $\vec{\sigma} \doteq (\sigma_x, \sigma_y, \sigma_z)$. The following irreducible unitary representation on \mathbb{C}^2 exists:

$$\begin{aligned} \mathcal{R}(i\sigma_\alpha) = \mathcal{R}(-i\sigma_\alpha) = \sigma_\alpha, & \quad \alpha = x, y, z \\ \mathcal{R}(I) = \mathcal{R}(-I) = I. & \end{aligned} \quad (13)$$

Using this representation, from the tomographic reconstruction formula (3) we obtain

$$\rho = \sum_{m=-1/2}^{1/2} \sum_{\alpha=x,y,z} p(\vec{n}_\alpha, m) m \sigma_\alpha + \frac{1}{2}. \quad (14)$$

Notice that, by using equation (14), it is sufficient to measure the spin in only three directions. Analogously, for spin $s = 1$ it is possible to find a finite group as an alternative to $SU(2)$. In fact, consider the 12-element tetrahedral group composed of the $\pm \frac{2}{3}\pi$ rotations around the vectors $\{\vec{n}_1 = \frac{1}{\sqrt{3}}(1, 1, 1), \vec{n}_2 = \frac{1}{\sqrt{3}}(1, -1, -1), \vec{n}_3 = \frac{1}{\sqrt{3}}(-1, 1, -1), \vec{n}_4 = \frac{1}{\sqrt{3}}(-1, -1, 1)\}$, of the π rotations around $\{\vec{n}_5 = (1, 0, 0), \vec{n}_6 = (0, 1, 0), \vec{n}_7 = (0, 0, 1)\}$ and of the identity. It induces a unitary irreducible representation on the space \mathbb{C}^3 , given by the 3×3 rotation

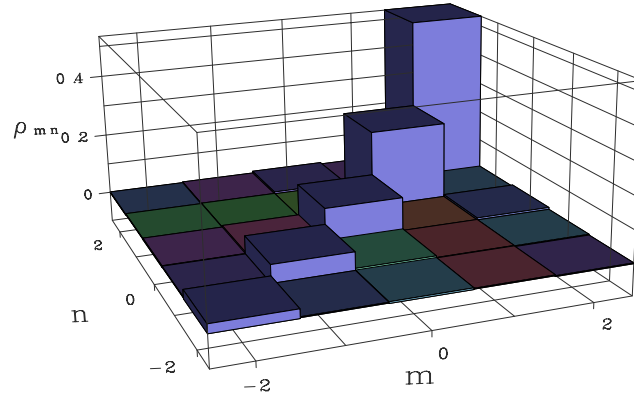


Figure 4. Density matrix for a thermal spin state ϱ_{th} . Here $\epsilon = 0.75$ and $s = 2$, and 60 000 simulated measurements have been used in the reconstruction.

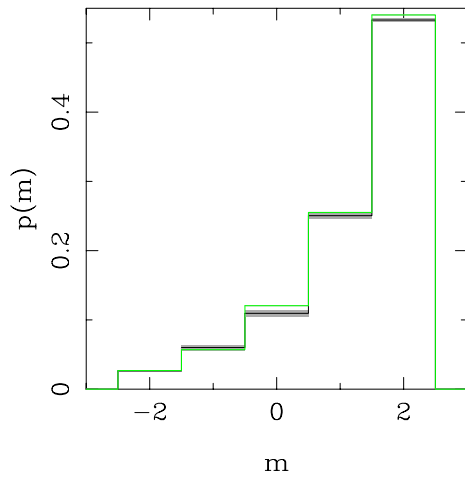


Figure 5. Main diagonal of the matrix given in figure 4. The error bars, which in this case are practically negligible, are obtained by dividing the measurements into 10 statistical blocks. The full line indicates the theoretical value.

matrices. Hence, equation (2) now becomes

$$\varrho = \frac{1}{4} \sum_{m=-1}^1 \sum_{j=1}^7 p(\vec{n}_j, m) \mathcal{K}_j(m - \vec{s} \cdot \vec{n}_j) + \frac{1}{4} I, \quad (15)$$

with

$$\mathcal{K}_j(x) = \begin{cases} 2 \cos(\frac{2}{3}\pi x) & j = 1, 2, 3, 4 \\ e^{-i\pi x} & j = 5, 6, 7. \end{cases} \quad (16)$$

Notice that this procedure does not make use of a minimal set of measurements, since 14 experimental parameters must be determined in (15), whereas there are only 8 independent real parameters in the 3×3 density matrix. In contrast, the case of spin $s = 1/2$ outlined previously does use the minimal set of measurements for such a system. In figure 6 a comparison between the two spin tomography procedures given by equations (6) and (15) is shown through a Monte Carlo simulation. Notice that there is no significant difference in the results, showing that there is no substantial need for a procedure which involves a minimal set of measurements.

For spins $s > 1$ an analogous procedure holds: one needs to find a finite group such that it induces an irreducible unitary representation on $\mathcal{H} = \mathbb{C}^{2s+1}$.

3. Many-particle spin tomography

The mathematical extension of the method to the case of a system composed of many spins is trivial, yet it predicts the necessity of performing measurements on single components and this may not always be possible when the system is composed of indistinguishable particles. For this reason, we need to develop the theory more.

3.1. Distinguishable spins.

As tomographic group for a system of N spins we can simply use $SU(2)^{\otimes N}$. Up to equivalences, its irreducible representations are given by the direct product of N operators (4) and the invariant measure is the product of N measures (5). As a consequence of the tomography reconstruction formula (3) applied to $SU(2)^{\otimes N}$, we readily attain the following generalization of equation (6):

$$\varrho = \prod_{k=1}^N \frac{(2s_k + 1)}{4\pi^2} \int_0^{2\pi} d\psi_k \sin^2 \frac{\psi_k}{2} \int_0^\pi d\vartheta_k \sin \vartheta_k \times \int_0^{2\pi} d\varphi_k \text{Tr}[\varrho e^{i\vec{s}_k \cdot \vec{n}_k \psi_k}] e^{-i\vec{s}_k \cdot \vec{n}_k \vartheta_k}, \quad (17)$$

where k is the particle index. The trace term in (17) gives rise to the probability $p(\vec{n}_1, m_1; \dots; \vec{n}_N, m_N)$ of obtaining m_k as a result for the measurement of the k th spin \vec{s}_k in the direction \vec{n}_k . This information is accessible only in the case of fully distinguishable spins.

In figure 7 a simulated tomographic reconstruction of the value of $\langle S_z \rangle$ (S_z being the total spin component in the z -direction) is given for different multiparticle spin states. Notice how the number of necessary experimental data increases exponentially with the number of spins, since the statistical error is exponential in the number of particles.

3.2. Indistinguishable spin-1/2 particles.

Suppose we were given a system of N particles with the same spin. Such particles may be treated as identical by introducing a new dynamical variable, as in the case of the isospin. The spin density matrix (which is the partial trace over the orbital degrees of freedom of the global density matrix) is completely symmetrical, i.e.

$$P\varrho P^{-1} = \varrho, \quad (18)$$

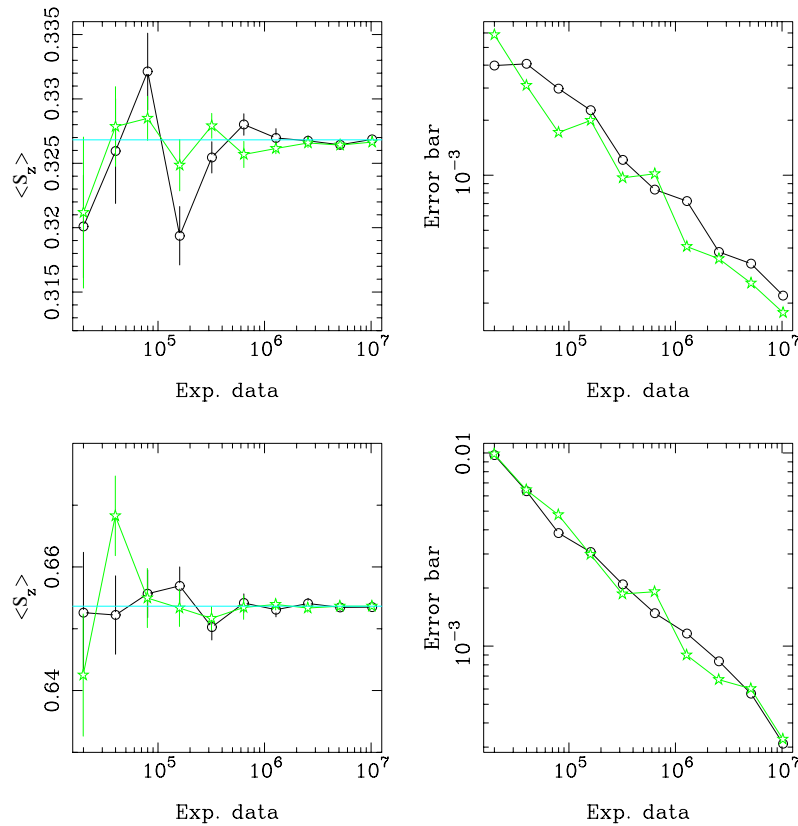


Figure 6. Monte Carlo comparison between continuous and discrete tomography. Continuous tomography uses $SU(2)$ as the tomographic group and is based on equation (6), while discrete tomography uses $SU(2)$ finite subgroups and is based on the reconstruction procedures given in equation (14) for $s = 1/2$ (utilizing, in this case, a minimal set of measurements) and equation (15) for $s = 1$. Left: convergence of the mean value of $\langle s_z \rangle$ for a coherent $\alpha = 2$ spin state for increasing numbers of experimental data (the theoretical value is given by the horizontal lines). The circles refer to continuous, and the stars to discrete, tomography. The upper graph is for spin $s = 1/2$ and the lower is for $s = 1$. Right: plots of the statistical error bars of the graphs on the left versus experimental data. The error bars are obtained by dividing the experimental data into 20 statistical blocks. Notice that the two tomographic procedures are essentially equivalent: they converge in the same way at the same result.

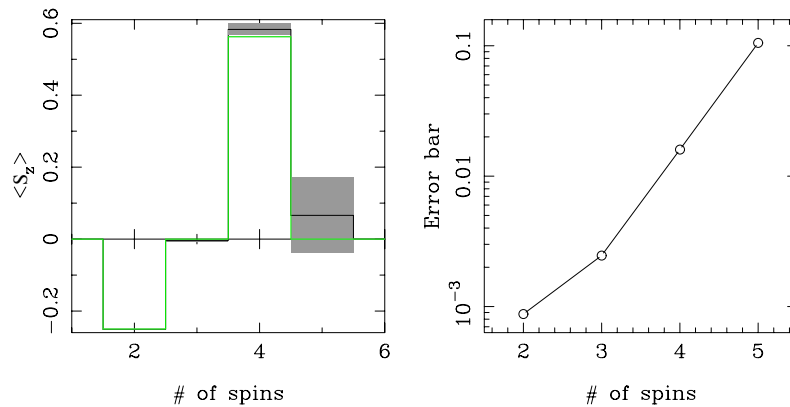


Figure 7. Left: plot of $\langle S_z \rangle$ for different numbers of spins in a completely symmetrical state. A total of 10^6 measurements for each mean value was performed in this simulation. Right: semilog plot of the error bars versus the number of spins. Notice the exponential increase in the statistical errors.

for any particle permutation P , because of the complete symmetry of the global density matrix.

It is also possible to see that the spin density matrix is block diagonal in the representation of vectors of definite symmetry, with the subspace corresponding to each block spanned by vectors belonging to the same symmetry. In fact, given $|\phi\rangle$ and $|\psi\rangle$ vectors of different symmetry types [8], then

$\langle \phi | \psi \rangle = 0$. Hence, for any operator ϱ , satisfying (18), one has $\langle \phi | \varrho | \psi \rangle = 0$, as $\varrho | \psi \rangle$ belongs to the same symmetry type as $|\psi\rangle$.

Since the square of the total spin S^2 and its z component S_z both commute with all permutation operators P , the common eigenvectors of S^2 and S_z may be taken as a base for each of the diagonal blocks of the spin matrix. Let us now restrict

our attention to $s = 1/2$ spin particles. In this case, for each symmetry type there corresponds only one value of S , where $S(S+1)$ is the eigenvalue of S^2 . In fact, given $[\lambda_1 \lambda_2]$ the partition of N which defines the class of permutations P that indicate a symmetry type, we find $S = \frac{1}{2}(\lambda_1 - \lambda_2)$ [9].

Let $\mathcal{H}_{S,M}$ be the space of vectors with assigned S and M (M being the eigenvalue of S_z). The spin density matrix restricted to $\mathcal{H}_{S,M}$, which is given by $\varrho_{S,M}$, is again completely symmetrical, hence $[P, \varrho_{S,M}] = 0$. Moreover, $\mathcal{H}_{S,M}$ is associated with an irreducible representation of the permutations group [9]. By using Schur's lemma, we can thus conclude that $\varrho_{S,M} \propto I$, I being the identity in $\mathcal{H}_{S,M}$. In $\mathcal{H}_{S,M}$ there may be vectors of different symmetry type i , yet $\langle i, S, M | \varrho_{S,M} | i, S, M \rangle$ does not depend on the index i , so that the probability for the measurement of S^2 and S_z does not depend on the symmetry type. The same conclusion holds for the measurement of S^2 and $\vec{S} \cdot \vec{n}$ for any vector \vec{n} . Hence, from the arbitrariness of \vec{n} , we conclude that blocks with the same S (and different symmetry type) are coincident.

In conclusion, we have proved that in the $\{S^2\}$ representation ϱ is block diagonal, that each block corresponds to a value of S and that blocks with the same S are equal. Remarkably, applying equation (2) to each block, we can reconstruct ϱ measuring only the global quantities S^2 and $\vec{S} \cdot \vec{n}$. Some examples will clarify both the theory and the needed experimental set-up.

In the case of two spins $1/2$, the spin density matrix will be of the form

$$\varrho = \begin{pmatrix} \sigma_{11} & \sigma_{12} & \sigma_{13} & 0 \\ \sigma_{21} & \sigma_{22} & \sigma_{23} & 0 \\ \sigma_{31} & \sigma_{32} & \sigma_{33} & 0 \\ 0 & 0 & 0 & \alpha \end{pmatrix} \doteq \sigma \oplus \alpha, \quad (19)$$

where the σ block corresponds to the subspace spanned by the eigenstates of $S = 1$ (which are symmetrical with respect to particle permutations), while the α block to the subspace spanned by the only eigenvector of $S = 0$ (antisymmetrical with respect to permutations). Applying (2) to each block one finds

$$\varrho = \int \frac{d\vec{n}}{4\pi} \sum_{M=-1}^1 p(S=1, \vec{S} \cdot \vec{n} = M) K_{s=1} \times (M - \vec{S} \cdot \vec{n}) \oplus p(S=0). \quad (20)$$

According to (20), in order to measure ϱ , we only need the probability distributions $p(S, \vec{S} \cdot \vec{n})$, corresponding to the operators S^2 and $\vec{S} \cdot \vec{n}$, for all \vec{n} , which can be suitably recovered using the apparatus depicted in figure 8, which will be analysed later.

Similarly, the spin density matrix of three spins $1/2$ is

$$\varrho = \begin{pmatrix} \xi_{11} & \xi_{12} & \xi_{13} & \xi_{14} & 0 & 0 & 0 & 0 \\ \xi_{21} & \xi_{22} & \xi_{23} & \xi_{24} & 0 & 0 & 0 & 0 \\ \xi_{31} & \xi_{32} & \xi_{33} & \xi_{34} & 0 & 0 & 0 & 0 \\ \xi_{41} & \xi_{42} & \xi_{43} & \xi_{44} & 0 & 0 & 0 & 0 \\ 0 & 0 & 0 & 0 & \pi_{11}^1 & \pi_{12}^1 & 0 & 0 \\ 0 & 0 & 0 & 0 & \pi_{21}^1 & \pi_{22}^1 & 0 & 0 \\ 0 & 0 & 0 & 0 & 0 & 0 & \pi_{11}^2 & \pi_{12}^2 \\ 0 & 0 & 0 & 0 & 0 & 0 & \pi_{21}^2 & \pi_{22}^2 \end{pmatrix}. \quad (21)$$

The ξ block corresponds to $S = 3/2$, whereas the π blocks both correspond to $S = 1/2$, and are distinguished by their different

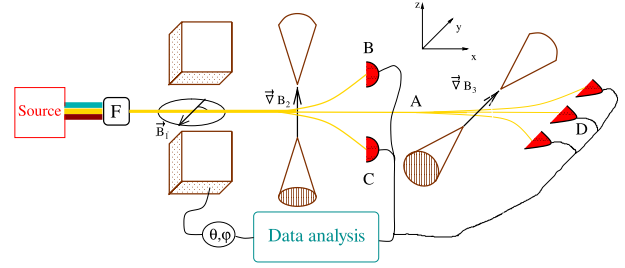


Figure 8. Experimental apparatus for the tomography of systems composed of two spins $1/2$.

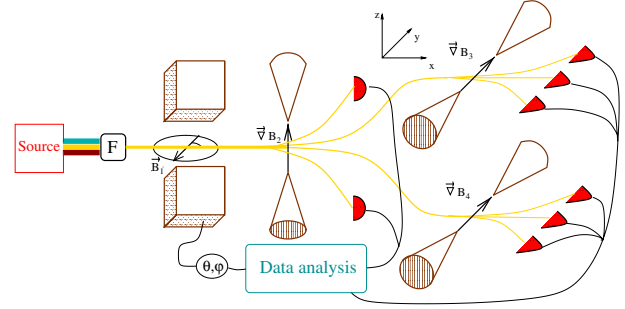


Figure 9. Experimental apparatus for the tomographic reconstruction of the spin states of systems composed of three spin- $1/2$ states.

symmetry properties. The argument presented previously proves that $\pi_{ij}^1 = \pi_{ij}^2$, for all i, j . Thus we can write $\varrho = \xi \oplus \pi \oplus \pi$, with $\pi \doteq \pi^1 = \pi^2$. Again, applying (2) to each block leads to

$$\xi = \int \frac{d\vec{n}}{4\pi} \sum_{M=-\frac{3}{2}}^{\frac{3}{2}} p\left(S = \frac{3}{2}, \vec{S} \cdot \vec{n} = M\right) K_{s=\frac{3}{2}}(M - \vec{S} \cdot \vec{n}), \quad (22)$$

$$\pi = \int \frac{d\vec{n}}{4\pi} \sum_{M=-\frac{1}{2}}^{\frac{1}{2}} \frac{1}{2} p\left(S = \frac{1}{2}, \vec{S} \cdot \vec{n} = M\right) K_{s=\frac{1}{2}}(M - \vec{S} \cdot \vec{n}), \quad (23)$$

and the problem of determining ϱ is again reconducted to the simultaneous measurement of S^2 and $\vec{S} \cdot \vec{n}$.

Both in the cases presented and in the general n -spins case, the required experimental data are the distributions $p(S, \vec{S} \cdot \vec{n})$. The apparatus to produce such data is basically equivalent in the two cases, as evident in figures 8 and 9. Hence we shall limit the analysis to the two-spins case. Here, the Fizeau filter and the magnetic field $\vec{B}_1 = B_1 \vec{n}_\perp = B_1(-\sin \varphi, \cos \varphi, 0)$ have the same purpose as in single-particle tomography (figure 1).

Consider a beam of n non-interacting systems composed of two particles with spin- $1/2$. As the analysis can be immediately extended to a mixed case, for simplicity let us consider each system in the pure state

$$|\Psi_o\rangle = \gamma^s |0, 0\rangle + \gamma_{-1}^a |1, -1\rangle + \gamma_0^a |1, 0\rangle + \gamma_1^a |1, 1\rangle, \quad (24)$$

with $|a, b\rangle$ standing for $|S = a, M = b\rangle$. The beam is split into three parts by the gradient \vec{B}_2 and the systems arrive in detector B with the apparatus of figure 8 with a probability $p(S=1, M=1) = |\gamma_1^a|^2$ and in detector C with a probability $p(S=1, M=-1) = |\gamma_{-1}^a|^2$. The remaining particles reach position A with a probability

$$p_A = |\gamma^s|^2 + |\gamma_0^a|^2 \quad (25)$$

and are left in the state

$$|\Psi_A\rangle = \frac{1}{p_A} \xi (\gamma^s |0, 0\rangle + \gamma_0^a |1, 0\rangle). \quad (26)$$

As the subsequent gradient is directed along the y axis, equation (26) is conveniently written using the eigenstates of S_y , i.e. $|S, M\rangle_y$:

$$|\Psi_A\rangle = \frac{1}{p_A} [\gamma^s |0, 0\rangle_y + \gamma_0^a \alpha_{-1} |1, -1\rangle_y + \gamma_0^a \alpha_0 |1, 0\rangle_y + \gamma_0^a \alpha_1 |1, 1\rangle_y], \quad (27)$$

where $\alpha_i \doteq {}_y\langle 1, i | 1, 0\rangle$ ($i = -1, 0, 1$). Hence, the probability for a system to arrive at detector D is

$$p_S = \frac{1}{p_A} [|\gamma^s|^2 + |\gamma_0^a|^2 |\alpha_0|^2]. \quad (28)$$

By measuring p_A and p_S , the quantities $|\gamma^s|^2$ and $|\gamma_0^a|^2$ are obtained by inverting equations (25) and (28). The coefficients $|\gamma_0^a|^2$, $|\gamma^s|^2$, $|\gamma_1^a|^2$ and $|\gamma_{-1}^a|^2$ are the four probabilities $p(S, M)$ we need for the reconstruction given by equation (20).

A similar argument shows that the equipment of figure 9 supplies $p(S, M)$, for all S, M , for a system constituted of three spins $1/2$.

4. Feasibility

The orders of magnitude of the experimental parameters are such that the experiment is feasible with currently available technology. Only as an example, consider the following cases of spin measurements of electrons or nucleons. For the magnet which is responsible for the field \vec{B}_1 with length of the order of 1 cm, we can measure the state of a beam of electrons with speed $\sim 10^9$ cm s $^{-1}$, by using a magnetic field $B_1 = \vartheta/\gamma t$ varying between 0 and ~ 30 G. On the other hand, in the nucleon case, choosing a speed of $\sim 10^7$ cm s $^{-1}$, we need B_1 ranging between 0 and $\sim 10^2$ – 10^3 G. Obviously, the parameters B_1 and t can be adjusted over a wide range, according to the experimental situation.

5. Conclusions

We have presented a tomographic experimental procedure for the measurement of the spin density matrix. The experimental scheme is a consequence of formula (2), which was proved using group theory. Through some Monte Carlo simulations, we have shown that the reconstruction can be achieved with high precision using a limited number of measurements. The extension of the procedure to the reconstruction of states of multiple spin systems has been given, both for distinguishable spins and for indistinguishable spin- $1/2$ particles. Finally, we have shown that the orders of magnitude for the experimental set-up are such that it can be implemented with currently available technology.

Acknowledgments

This work has been sponsored by the INFM through project PRA-2002-CLON and by the EEC through project IST-2000-29681 (ATESIT).

Appendix. Group derivation of quantum tomography

The proof of equation (3) is obtained from the following lemma.

Lemma. *Let A be an arbitrary trace-class operator on the Hilbert space \mathcal{H} of the system and \mathcal{R} an irreducible unitary square integrable representation on \mathcal{H} of the tomographic group G . Then*

$$\text{Tr } A = \int dg \mathcal{R}(g) A \mathcal{R}^\dagger(g), \quad (A.1)$$

where dg is an invariant measure for the group G , normalized as $\int dg |\langle u | \mathcal{R}(g) | v \rangle|^2 = 1$ which is independent of the choice of the vectors $|u\rangle, |v\rangle \in \mathcal{H}$.

Proof. By using the unitarity of \mathcal{R} and the properties of group representations, we can write for any $h \in G$

$$\begin{aligned} \int dg \mathcal{R}(g) |u\rangle \langle v | \mathcal{R}^\dagger(g) \mathcal{R}(h) &= \int dg' \mathcal{R}(hg') |u\rangle \langle v | \mathcal{R}^\dagger(g') \\ &= \mathcal{R}(h) \int dg' \mathcal{R}(g') |u\rangle \langle v | \mathcal{R}^\dagger(g'), \end{aligned} \quad (A.2)$$

which, through Schur's lemma, guarantees that

$$\int dg \mathcal{R}(g) |u\rangle \langle v | \mathcal{R}^\dagger(g) = \tau_{u,v} I_{\mathcal{H}}, \quad (A.3)$$

$I_{\mathcal{H}}$ being the identity in \mathcal{H} . Consider the quantity

$$\int dg |\langle u | \mathcal{R}(g) | v \rangle|^2 = \tau_{v,v}, \quad (A.4)$$

where $|u\rangle$ and $|v\rangle$ are arbitrary normalized vectors in \mathcal{H} . From equation (A.3) it is trivial to see that $\tau_{v,v}$ is independent of $|u\rangle$. One can check that it is also independent of $|v\rangle$ by noticing that, given an arbitrary vector $|a\rangle$,

$$\begin{aligned} \tau_{v,v} &= \int dg \mathcal{R}(g) |v\rangle \langle v | \mathcal{R}^\dagger(g) = \int dh \mathcal{R}(h^{-1}) |v\rangle \langle v | \mathcal{R}^\dagger(h^{-1}) \\ &= \int dh \mathcal{R}(h) |a\rangle \langle a | \mathcal{R}^\dagger(h) = \tau_{a,a}, \end{aligned} \quad (A.5)$$

where the group unimodularity has been used in $dg = dh$ with $h \doteq g^{-1}$. Notice that the hypothesis of square-integrability of the representation guarantees the convergence of the integral in (A.4). Thus, the natural choice for the normalization of the group's measure is to take $\tau_{u,v} = 1$. The constant $\tau_{u,v}$ can be expressed in terms of $\tau_{v,v}$ by noticing that, upon taking $h \doteq g^{-1}$, one has

$$\begin{aligned} 1 &= \tau_{v,v} = \int dg \langle b | \mathcal{R}(g) | a \rangle \langle a | \mathcal{R}^\dagger(g) | b \rangle \\ &= \int dh \frac{\langle a | \mathcal{R}(h) | u \rangle \langle v | \mathcal{R}^\dagger(h) | a \rangle}{\langle v | u \rangle} = \frac{\tau_{u,v}}{\langle v | u \rangle}. \end{aligned} \quad (A.6)$$

The lemma's thesis is now easily found by using the Schmidt decomposition of A as $A = \sum_i \alpha_i |u_i\rangle \langle v_i|$:

$$\begin{aligned} \int dg \mathcal{R}(g) A \mathcal{R}^\dagger(g) &= \sum_i \alpha_i \int dg \mathcal{R}(g) |u_i\rangle \langle v_i | \mathcal{R}^\dagger(g) \\ &= \sum_i \alpha_i |v_i\rangle \langle u_i| = \text{Tr } A. \end{aligned} \quad (A.7)$$

□

Group tomography theorem. *Let A be an arbitrary trace-class operator on the Hilbert space \mathcal{H} of the system and \mathcal{R} an irreducible unitary square integrable representation on \mathcal{H} of the tomographic group G . Then*

$$A = \int dg \operatorname{Tr}[A\mathcal{R}(g)]\mathcal{R}^\dagger(g). \quad (\text{A.8})$$

Proof. Let O be an invertible trace-class operator, it follows that $\mathcal{R}(g)O$ is trace-class for any $g \in G$. Hence it is possible to obtain, by applying (A.1) twice,

$$\int dg \operatorname{Tr}[A\mathcal{R}(g)]O\mathcal{R}^\dagger(g) = \int dg' \operatorname{Tr}[\mathcal{R}^\dagger(g')O]\mathcal{R}(g')A. \quad (\text{A.9})$$

Taking a basis $\{|k\rangle\}$ in \mathcal{H} , one can obtain, using again lemma (A.1),

$$\begin{aligned} & \int dg \operatorname{Tr}[\mathcal{R}^\dagger(g)O]\langle i|\mathcal{R}(g)A|j\rangle \\ &= \int dg \sum_k \langle k|\mathcal{R}^\dagger(g)O|k\rangle \langle i|\mathcal{R}(g)A|j\rangle \\ &= \sum_k \langle k|O \operatorname{Tr}[|k\rangle\langle i|]A|j\rangle = \langle i|OA|j\rangle. \end{aligned} \quad (\text{A.10})$$

From equations (A.9) and (A.10) it follows immediately that $\int dg \operatorname{Tr}[A\mathcal{R}(g)]O\mathcal{R}^\dagger(g) = OA$, which yields the thesis (A.8) by multiplying to the left both members by O^{-1} . \square

It is trivial to extend theorem (A.8) to the case of projective representations, i.e. group representations for which, given $g_1, g_2, g_3 \in G$ such that $g_1 \cdot g_2 = g_3$, one has

$$\mathcal{R}(g_1)\mathcal{R}(g_2) = e^{i\zeta(g_1, g_2)}\mathcal{R}(g_3), \quad (\text{A.11})$$

$\zeta \in \mathbb{R}$ being a phase factor depending on g_1 and g_2 . Notice, moreover, that the theorem here presented is valid also for discrete and finite groups, with the sum on group elements replacing the integral. From the result (A.8), with an appropriate choice for the tomographic group and the irreducible representation, it is possible to prove the formula for spin tomography (2)—derived in the following

section—and for optical homodyne tomography (1). Notice that the unimodularity hypothesis given in the definition of tomographic group G can be relaxed without losing most of the results we give in this paper.

References

- [1] D'Ariano G M 2000 *Phys. Lett. A* **268** 151
D'Ariano G M, Maccone L and Paris M G A 2000 *Phys. Lett. A* **276** 25
D'Ariano G M, Maccone L and Paris M G A 2001 *J. Phys. A: Math. Gen.* **34** 93
- [2] Amiet J-P and Weigert S 1999 *J. Phys. A: Math. Gen.* **32** L269
Weigert 1999 *Preprint* quant-ph/9904095
Newton R G and Young B-L 1968 *Ann. Phys., NY* **49** 393
Leonhardt U 1995 *Phys. Rev. Lett.* **74** 4101
Leonhardt U 1996 *Phys. Rev. A* **53** 2998 and references therein
Wootters W K 1986 *Found. Phys.* **16** 391
Opatrný T, Welsch D-G and Bužek V 1996 *Phys. Rev. A* **53** 3822
Band W and Park J L 1979 *Am. J. Phys.* **47** 188
Band W and Park J L 1971 *Found. Phys.* **1** 339
Brif C and Mann A 1999 *Phys. Rev. A* **59** 971
Andreev V A and Man'ko V I 2000 *J. Opt. B: Quantum Semiclass. Opt.* **2** 122
Dodonov V V and Man'ko V I 1997 *Phys. Lett. A* **229** 335
- [3] Smithey D T, Beck M, Raymer M G and Faridani A 1993 *Phys. Rev. Lett.* **70** 1244
D'Ariano G M, Leonhardt U and Paul M 1995 *Phys. Rev. A* **52** R1801
- [4] D'Ariano G M, Leonhardt U and Paul M 1995 *Phys. Rev. A* **52** R1801
D'Ariano G M 1997 *Measuring quantum states* *Quantum Optics and the Spectroscopy of Solids* ed T Hakioglu and A S Shumovsky (Dordrecht: Kluwer) p 175
- [5] D'Ariano G M, Maccone L and Paris M G A 2000 *Phys. Lett. A* **276** 25
D'Ariano G M, Maccone L and Paris M G A 2001 *J. Phys. A: Math. Gen.* **34** 93
- [6] Wigner E 1959 *Group Theory and its Application to the Quantum Mechanics of Atomic Spectra* (New York: Academic) p 167 formula (15.27)
- [7] Perelomov A M 1972 *Commun. Math. Phys.* **26** 222
Rasetti M 1973 *Int. J. Theor. Phys.* **13** 425
- [8] Hamermesh M 1962 *Group Theory* (New York: Addison-Wesley) ch 7
- [9] Messiah A 1961 *Quantum Mechanics* (Amsterdam: North-Holland) appendix D